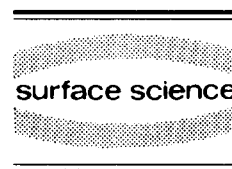




ELSEVIER

Surface Science 323 (1995) 295–303



Initial stages of SiGe epitaxy on Si(001) studied by scanning tunneling microscopy

A. Oral ^{*,1}, R. Ellialtıoglu

Department of Physics, Bilkent University, 06533 Ankara, Turkey

Received 18 August 1994; accepted for publication 7 October 1994

Abstract

We have studied the initial stages of strained SiGe alloy growth on the Si(001)-(2 × 1) surface by scanning tunneling microscopy. The Si_{0.36}Ge_{0.64} alloy was grown on the silicon substrate at various coverages (0.13–3.6 ML) and at different temperatures (~310–470°C). The growth was one dimensional, preferring the direction perpendicular to the underlying silicon dimer rows at low coverages and low temperatures. Anti-phase boundaries were observed to lead multi-layer growth. Strong interaction between the overlayer and the substrate was found to buckle the substrate as well as SiGe dimers. Different growth mechanisms, island formation and step flow, were identified at low and high substrate temperatures. (2 × n) ordering of the strained overlayer was only observed at an intermediate growth temperature (~390°C).

Keywords: Epitaxy; Scanning tunneling microscopy; Silicon; Silicon–germanium

1. Introduction

The epitaxial growth of Si_{1-x}Ge_x alloy on silicon substrates by using molecular beam epitaxy (MBE) and chemical vapour deposition (CVD) has become a very important issue over the last few years. Si and Ge form solid solutions at almost all compositions. Since the lattice constant of bulk Ge is 4.3% larger than Si, SiGe alloys grown on Si substrates are strained. However, the strain is relaxed if the thickness of the grown layer exceeds the critical thickness

which depends on the concentration. Growth of this technologically as well as scientifically important alloy has been extensively studied by various groups using different techniques [1–5]. This material system has attracted much attention for the potential opto-electronic applications [6]. Very high electron mobilities and the fractional quantum Hall effect have been observed in the strained Si layers grown between relaxed SiGe layers [7–9]. Ordering of the Si and Ge atoms within the alloy has been predicted [10], observed by various groups [3–5] and it is still subject of controversy [11]. Since the SiGe alloy system is compatible with the existing silicon micro-fabrication technology, it represents a challenging alternative to III–V semiconductor based device technology and recently, high speed commercial applications have started to emerge from SiGe based devices [12].

^{*} Corresponding author.

¹ Present address: School of Physics, University of Bath, Claverton Down, BA2 7AY, Bath, UK. E-mail: a.oral@midge.bath.ac.uk.

Recently silicon homoepitaxy on Si(001) [13–15] and germanium heteroepitaxy on Si(001) [13,16,17] have been investigated in detail using scanning tunneling microscopy (STM) by various groups. These experiments lead to better understanding of surface diffusion and epitaxial growth at the atomic scale. Although epitaxial growth of $\text{Si}_{1-x}\text{Ge}_x$ on Si has been extensively studied, the early stages of $\text{Si}_{1-x}\text{Ge}_x$ growth on Si(001) at the atomic level is still not well understood.

In this work we have analysed the initial stages of SiGe epitaxial growth on the Si(001) surface as a function of coverage and temperature using scanning tunneling microscopy (STM) for the first time. We have observed that the alloy grows pseudomorphically by island formation at low substrate temperature, $T_s = 310^\circ\text{C}$. The step flow mechanism takes over at high growth temperature, $T_s = 470^\circ\text{C}$. However, at an intermediate growth temperature of $T_s = 390^\circ\text{C}$, the alloy has been observed to be growing partially relaxed by $2 \times n$ ordering of the overlayer.

2. Experimental details

The experiments were performed in a ultra high vacuum (UHV) system with a base pressure of $< 3 \times 10^{-10}$ Torr. The UHV system has been built in our laboratory [18] and is equipped with STM, Auger

electron spectroscopy (AES), low-energy electron diffraction (LEED) for surface analysis, an e-beam heater and Si and Ge evaporation sources for the sample preparation. A fast-entry load-lock chamber allows easy exchange of tips and samples. The STM used in this study was a home-made instrument with a single tube scanner and a two-axis stick-slip coarse positioner, which is described in detail elsewhere [19]. 6×8 mm Si(001) samples were cut from commercially available [20] $525 \mu\text{m}$ thick, n-type wafers with $1\text{--}10 \Omega \cdot \text{cm}$ resistivity and misoriented 0.5° towards the [110] direction. This vicinal angle gives an average terrace size of around 160 \AA , which was confirmed by the STM results. The Si(001) samples were first degreased and cleaned with a wet-chemical oxide etch–regrowth procedure [21] and mounted on degassed tantalum sample holders before introducing them into the UHV chamber. The samples were degassed in the UHV for approximately 10 h at $\sim 680^\circ\text{C}$ by using an e-beam heater. An atomically flat, (2×1) reconstructed Si(001) surface was obtained after heating the sample briefly to $\sim 900^\circ\text{C}$ in situ to remove the final oxide layer. This procedure routinely gave well ordered and contamination-free Si(001) (2×1) surfaces as observed by LEED, STM and AES. Fig. 1 shows a high resolution STM image of a typical Si(001) (2×1) surface prepared by this recipe. The clean Si(001) surface has a small number of defects and most of the dimers are observed to be symmetric. It is well known that even an extremely

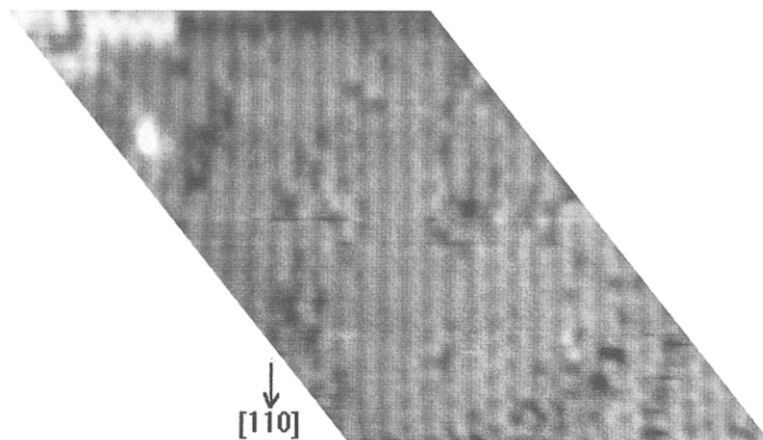


Fig. 1. STM image of Si(001) (2×1) surface. The sample voltage and tunneling current are -2 V and 1 nA , respectively.

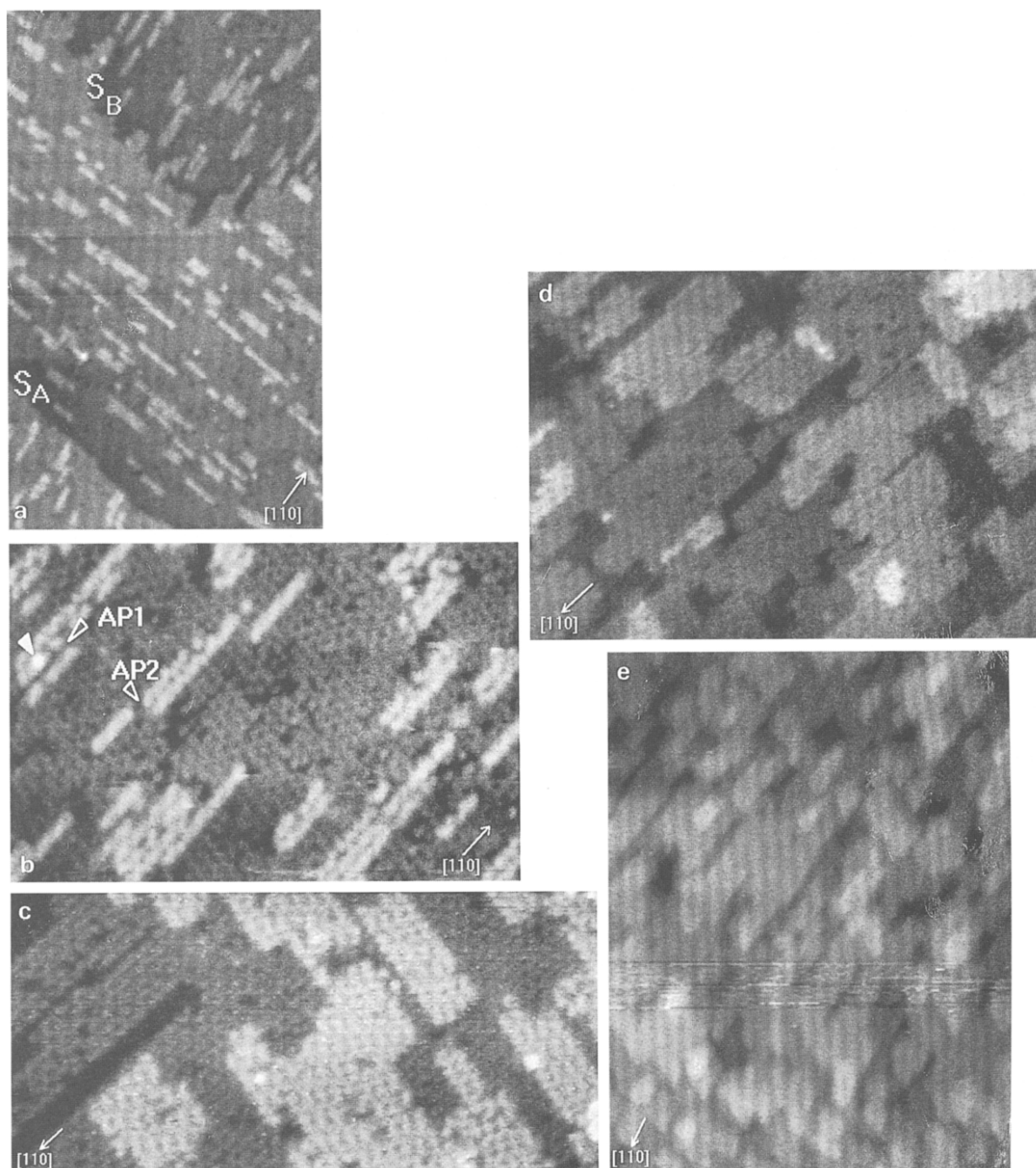


Fig. 2. Epitaxial growth of $\text{Si}_{0.36}\text{Ge}_{0.64}$ on $\text{Si}(001)$ at $T_s = 310^\circ\text{C}$ observed by STM. Coverages: (a) 0.13, (b) 0.25, (c) 0.8, (d) 1.6, and (e) 3.5 ML. Images sizes: (a) $\sim 640 \times 1000$, (b) $\sim 340 \times 230$, (c) $\sim 390 \times 185$, (d) $\sim 490 \times 340$, and (e) $\sim 770 \times 960$ Å. The S_A and S_B type steps are shown in (a). Antiphase boundaries, AP1 and AP2 are displayed in (b). The multilayer growth around AP1 is marked by a triangle on (b).

low amount of some impurity like Ni, causes a $(2 \times n)$, $n \approx 8$, reconstruction on the Si(001)(2×1) surface. We have never observed the influence of such impurities on Si(001) substrates cleaned with our recipe, which would have also affected the SiGe epitaxy.

Silicon and germanium were evaporated from separate home-made sources, which were composed of directly heated pieces of Si wafer and germanium granules held in tungsten baskets. The sources were water-cooled in order to reduce the outgassing of that part of the chamber. The evaporation rates of the silicon and germanium sources were calibrated using the STM itself by counting the islands grown on the Si(001) surface. Rate calibration was carried out at a low substrate temperature, $T_s = 200^\circ\text{C}$, to minimise the number of atoms incorporating into the steps. The concentration of the alloy was then calculated using the evaporation rates of the silicon and germanium sources. The $\text{Si}_{0.36}\text{Ge}_{0.64}$ alloys were grown on Si(001)(2×1) substrates at various coverages and at different temperatures. This alloy composition has been chosen randomly. The effect of alloy composition on the structure of the epitaxial layer will be the subject of a further study. The growth rate was kept fixed at 0.2 ML/min throughout the experiments and different $\text{Si}_{0.36}\text{Ge}_{0.64}$ coverages were obtained by increasing the exposure time of the sample. A new sample was used for each experiment.

An infrared pyrometer was used for temperature measurement in the high temperature range. In addition, a K-type thermocouple mounted at the center of a Si sample was used to calibrate the heater at low temperatures and the heater input power was then used to deduce the substrate temperatures. Samples as well as sample holders used in the experiments were of the same size in order to achieve temperature reproducibility. Tungsten tips prepared from a 0.2 mm diameter wire by electrochemical etching in KOH solution floated on CCl_4 were degreased and used without any further in situ treatment. These tips were used as long as they gave atomic resolution. STM images presented in this work were recorded with a negative sample bias of 2 V, thus imaging the filled sample states. The empty state imaging was rarely used throughout our experiments. Tunneling currents between 0.25 and 1 nA were used throughout the experiments.

3. Results

Fig. 2 shows the STM images of $\text{Si}_{0.36}\text{Ge}_{0.64}$ grown on Si(001) samples at various coverages from 0.13 to 3.5 ML. These samples were grown at a relatively low substrate temperature of 310°C . At very low coverage, $\theta = 0.13$ ML, the growth was highly anisotropic as shown in Fig. 2a and the alloy grew almost as one dimer wide “strings” oriented perpendicular to the underlying Si dimer rows. The dimerization direction of the grown layer is not surprising, because the successive layers of the Si(001) are reconstructed orthogonal to each other. Isolated dimers, as well as wider islands were also observed to have grown on the substrate. The same behaviour was also observed in our evaporation source calibration experiments, Si on Si(001) and Ge on Si(001). This anisotropy arises due to a sticking coefficient which is much larger at the end of the dimer rows than along the dimer rows [13]. Furthermore, the formation energy of S_A type steps is lower than that of S_B type [22] and the anisotropic growth of the islands perpendicular to the underlying Si(001) dimer rows is also thermodynamically preferred. Diffusion of a Si or a Ge atom along the substrate dimer rows on the surface is much easier than in the perpendicular direction [23]. However, this cannot suppress the observed anisotropy since the diffusion along the steps and the sticking coefficient at the end of the dimer rows are also high and the migrating atoms prefer to incorporate at the end of the dimer rows. Moreover, the S_A type steps were observed to be better sinks for the evaporated Si and Ge atoms migrating on the lower terrace compared to the ones on the upper terrace, as can be seen from uneven denuded zones around these steps in Fig. 2a. However, S_B type steps were equivalent sinks for the atoms migrating on both of the terraces, because the denuded zones around these steps were almost equal [13].

The shape anisotropy was reduced and wider islands perpendicular to the dimer rows began to grow as the coverage was increased to $\theta = 0.26$ ML as shown in Fig. 2b. The formation of antiphase boundaries can be observed even at this coverage when two islands meet and if the dimers in these neighbouring islands were out of phase by one unit cell of the unreconstructed Si substrate. There were

two types of antiphase boundaries (AP) on the overlayer. AP1 forms when two different phase islands meet along the dimer rows as can be seen in Fig. 2b.

On the other hand, AP2 is formed if those islands met at the end of the dimer rows. Multilayer growth of the alloy has been observed to be promoted by

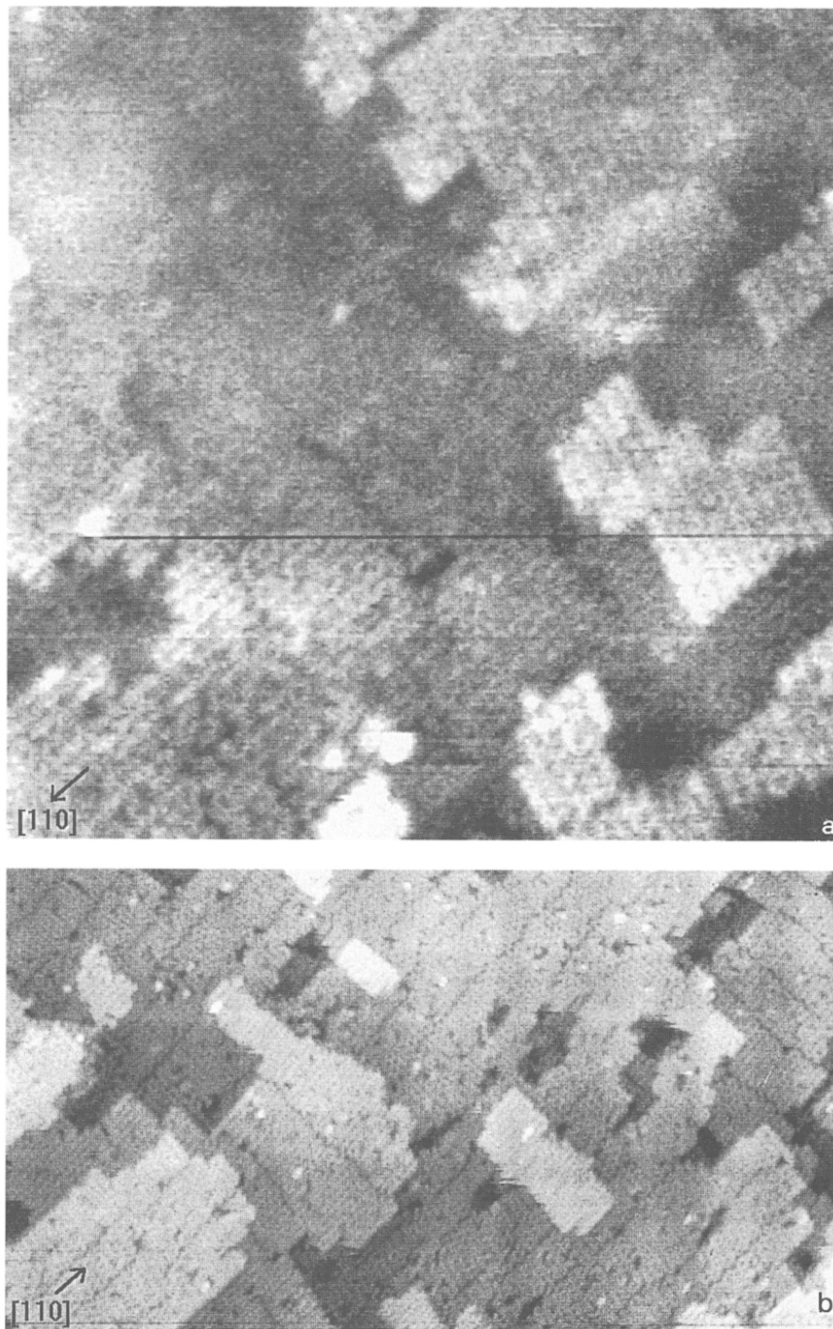


Fig. 3. Growth of $\text{Si}_{0.36}\text{Ge}_{0.64}$ on $\text{Si}(001)$ at $T_s = 390^\circ\text{C}$ observed by STM. Film thicknesses: (a) 0.5, and (b) 3.5 ML. Fields of view : (a) $\sim 390 \times 390$, and (b) $\sim 815 \times 450$ Å.

these antiphase boundaries as pointed out in Fig. 2b. Another interesting feature was the complete buckling of the silicon substrate dimers as can be seen in Figs. 2b and 2c. This leads to change in the reconstruction from (2×1) symmetric to $c(4 \times 2)$ anti-

symmetric (buckled) configuration [17]. Moreover, the dimer structure of the epitaxial alloy is symmetric if the islands are one dimer wide and buckled otherwise [14].

The energy difference between the symmetric and

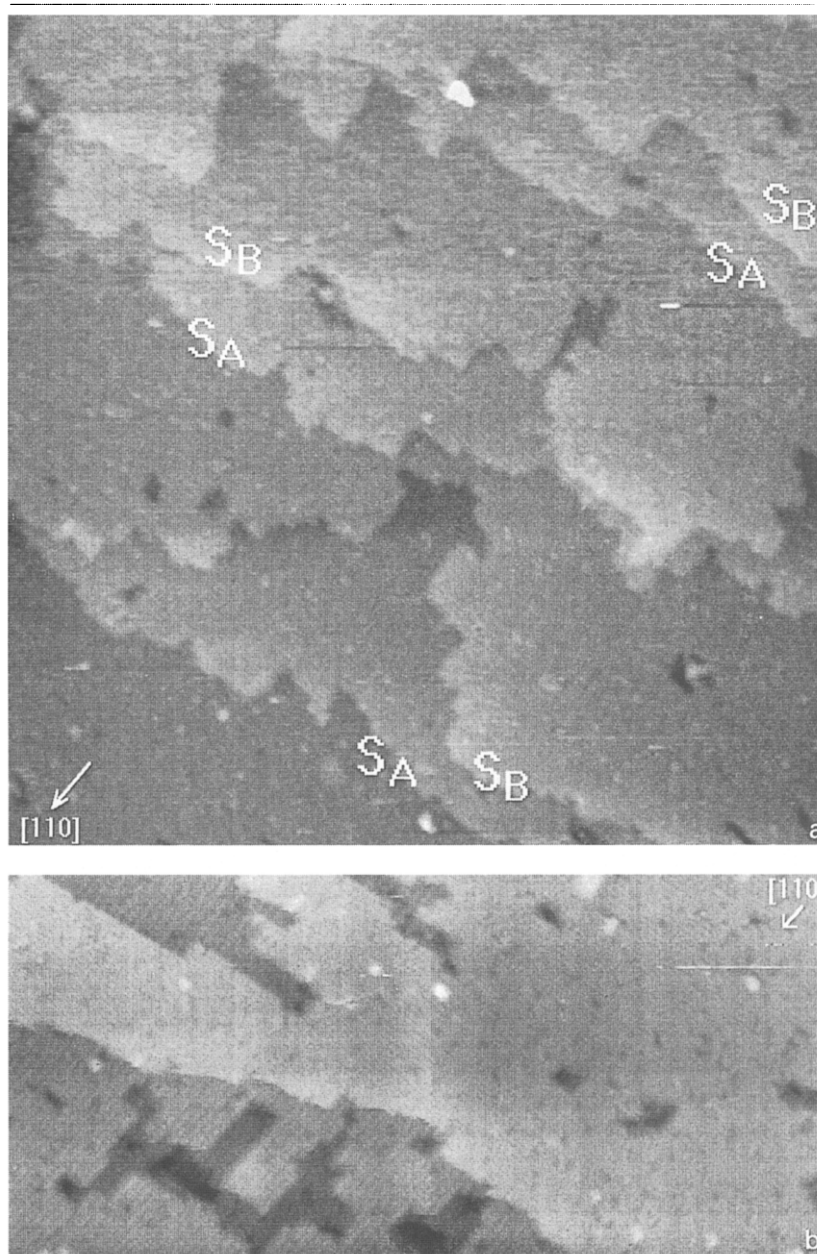


Fig. 4. STM image of (a) 0.8 ML and (b) 3.5 ML $\text{Si}_{0.36}\text{Ge}_{0.64}$ grown on Si(001) at $T_s = 470^\circ\text{C}$. Images sizes : (a) $\sim 1950 \times 1950$, and (b) $\sim 725 \times 340 \text{ \AA}$. The S_A and S_B type steps are marked in (a).

the buckled dimers on the Si(001) surface is very small, and either defects, thermal excitations [24] or tip-sample interactions affect the appearance of the dimers [25]. In this work, the compressive strain in the alloy was partially transmitted to the substrate and this interaction increases the energy difference between two equivalent configurations of the buckled dimers on the substrate such that it can no longer be suppressed by tip-sample interactions or thermal excitations. It should be pointed out that even though the strain in the $\text{Si}_{0.36}\text{Ge}_{0.64}$ should be substantially lower than for epitaxial Ge on Si(001) [17], it is still sufficient to buckle the silicon substrate dimers completely.

Further growth of the SiGe alloy resulted in the merging of the 2D islands with themselves and with the substrate steps. Fig. 2c shows the STM image of 0.8 ML $\text{Si}_{0.36}\text{Ge}_{0.64}$ grown on Si(001) under the same experimental conditions. The second epitaxial layer has started to grow before the first layer was completed. Another interesting observation was the lack of $(2 \times n)$, $n \geq 8$, reconstruction on the overlayer grown at this temperature. $(2 \times n)$ reconstruction of the thick $\text{Si}_{0.5}\text{Ge}_{0.5}$ layers grown on Si(001) by MBE has been observed by Butz and Kempers [26].

When the coverage was increased to $\theta = 1.6$ ML, the first overlayer was still not complete, as shown in Fig. 2d. The SiGe islands just met one another and merged on the substrate and then combined with the substrate steps. Even the third layer has started to grow at the expense of the first and the second layers. At this low growth temperature, $T_s = 310^\circ\text{C}$, the number of antiphase boundaries was quite high. Once they were established, they formed a low quality substrate for the subsequent overlayers and substrate steps on the surface became difficult to distinguish at this coverage.

At 3.5 ML coverage, as can be seen in Fig. 2e, the first SiGe layer was almost complete, but there were still some patches left empty. The growth has involved in a number of different layers. It was still two dimensional, but the epitaxial layer quality was quite low due to multilayer growth promoted by the antiphase boundaries.

The $\text{Si}_{0.36}\text{Ge}_{0.64}$ alloy was also grown at higher substrate temperatures in order to understand the effect of T_s on epitaxy. At an intermediate substrate

temperature, $T_s = 390^\circ\text{C}$, the surface diffusion length was considerably higher than that at $T_s = 310^\circ\text{C}$. However, the growth still occurred via island formation at this temperature and the step-island and the island-island interactions were observed to be affecting the growth. Fig. 3a shows the STM image of 0.5 ML $\text{Si}_{0.36}\text{Ge}_{0.64}$ grown on Si(001) substrate at $T_s = 390^\circ\text{C}$. In contrast to the lower temperature growth, $2 \times n$ ordering of the SiGe epitaxial layer was observed at this substrate temperature. The alloy was partially relaxed by formation of missing dimer rows which lead to $2 \times n$ reconstruction of the alloy. At this temperature, the SiGe overlayer, as well as the silicon substrate dimers were fully buckled as was found for the lower temperature growth. Further increase in the coverage to $\theta = 3.5$ ML resulted in the complete $2 \times n$ reconstruction of the overlayer as shown in Fig. 3b. The growth was again multi-layered as at the low substrate temperature but the number of layers contributing to the growth process was considerably reduced. Another prominent feature was the $2 \times n$ reconstruction of each contributing SiGe overlayer. The defect density is much lower as compared to the previous case and the growth takes place in relatively few layers because of the higher diffusion coefficient at this substrate temperature.

At a yet higher substrate temperature of $T_s = 470^\circ\text{C}$, the growth was mainly via step flow rather than island formation in contrast to the previous cases. Fig. 4a shows 0.8 ML of $\text{Si}_{0.36}\text{Ge}_{0.64}$ grown on Si(001) at this relatively high substrate temperature. There were no isolated SiGe islands left on the surface, all of them having merged with the steps due to the very high surface diffusion. Unequal terrace widths suggest that the growth was mainly accomplished by S_B type steps. The similarity of successive S_A and S_B step patterns is worth to pay further attention. This might be due to competition between single and double steps during the growth [15,22]. At a higher alloy coverage of 3.5 ML, very wide SiGe islands were observed as shown in Fig. 4b, however, the overlayer was still of high quality. This slight change in the growth mechanism from step flow can be due to increase in the overlayer thickness as well as the known segregation of Ge towards the surface [26]. There were also virtually no anti-phase boundaries present on the surface at this growth temperature. However, no $2 \times n$ reconstruc-

tion was observed at this temperature in contrast to $T_s = 390^\circ\text{C}$.

4. Conclusions

In this work, $\text{Si}_{0.36}\text{Ge}_{0.64}$ epitaxial layers have been grown on the $\text{Si}(001)(2 \times 1)$ surface in UHV at various coverages ($\theta \approx 0.13\text{--}3.5$ ML) and substrate temperatures $T_s = 310\text{--}470^\circ\text{C}$. The growth was found to be highly anisotropic, and the preferred direction of the growth was perpendicular to the underlying dimer rows of the $\text{Si}(001)(2 \times 1)$ substrate. Antiphase boundaries started to appear as the alloy coverage on the substrate was increased at the lower substrate temperatures. These antiphase boundaries were observed to promote multilayer growth of the alloy before an atomic layer had been completely grown, resulting in a poor epitaxial layer quality. Higher coverages led to enhanced multilayer growth involving a number of monolayers. At low substrate temperatures, $T_s = 310\text{--}390^\circ\text{C}$, growth occurred via island formation and the coalescence of the islands with one another and with the steps. However, at a higher temperature, $T_s = 470^\circ\text{C}$, the growth was effectively taking place via step flow due to the enhanced diffusion of the surface atoms. It has also been observed that one of the steps, namely S_B , grows much faster than the S_A type steps at higher T_s . Moreover, S_B type steps have been observed to be symmetric sinks for the atoms diffusing on upper and lower terraces, while the S_A type steps were found to be a better sink for the atoms diffusing on the lower terrace than on the upper terrace.

Another interesting result was the strong interaction of the strained SiGe epitaxial layer with the silicon substrate. The strain in the overlayer changes the structure of the dimers on the $\text{Si}(001)$ from (2×1) symmetric to $c(4 \times 2)$ antisymmetric (buckled) configuration. Moreover, the epitaxial overlayer dimers have been observed to be completely buckled.

One of the most interesting results was the $(2 \times n)$ reconstruction of the alloy which has only been observed at an intermediate substrate temperature, $T_s = 390^\circ\text{C}$. At low substrate temperatures, $T_s = 310^\circ\text{C}$, the Si and Ge atoms landing on the surface cannot migrate very long distances and interact with

one another and with the steps, they instead freeze on the surface relatively quickly. On the other hand, at high growth temperatures, $T_s = 470^\circ\text{C}$, the diffusion length for the atoms arriving at the substrate is larger than the terrace width so that they can easily reach the steps, migrate along and incorporate at these energetically favourable sites. At an intermediate temperature, $T_s = 390^\circ\text{C}$, however, the diffusion length of the landing atoms are smaller than the average terrace size but sufficiently large to interact with the other migrating atoms and existing SiGe islands. Therefore, they can reach a configuration having a lower energy, which is observed to be the formation of missing dimer rows, resulting in $2 \times n$ ordering of the alloy. $2 \times n$ reconstruction of the SiGe alloy is a metastable phase of the system, which may be visualised as a local minimum in the Born–Oppenheimer surface describing the alloy system. Therefore, lower and higher growth temperatures result in different configurations, which is consistent with our observations. On the other hand, segregation of Ge towards the surface [26] is a well established phenomenon during SiGe growth. Therefore, we would expect a higher Ge concentration in the outermost layers of the SiGe alloy. This might have some influence on the $2 \times n$ ordering of the SiGe layers at $T_s = 390^\circ\text{C}$ [27].

Although the experiments were carried out under various tunneling conditions, a contrast between the Si and the Ge atoms which constitute the alloy has not yet been observed. We have recently performed number of filled/empty state imaging to distinguish between Si and Ge atoms, but no solid data has been obtained so far. However, we believe that more detailed experiments, particularly those using scanning tunneling spectroscopy together with the STM, would eventually reveal a contrast between Si and Ge atoms. Further experiments are necessary to understand the mechanisms of ordering, segregation and composition fluctuations in $\text{Si}_{1-x}\text{Ge}_x$ alloys which have been predicted [10] and observed by different methods on a coarse scale [3–5,11]. Different diffusion and sticking coefficients for Si and Ge atoms on the surface are expected to result in very interesting growth schemes and alloy atomic structures.

In summary, we have studied the initial stages of strained SiGe epitaxy on the $\text{Si}(001)(2 \times 1)$ surface

using STM for the first time. Strong anisotropy in the growth has been observed under various growth conditions. In addition, interaction between the substrate and the highly strained SiGe alloy has also been observed to result in complete buckling of the substrate as well as the overlayer itself. Moreover, different growth mechanisms have been identified at different substrate temperatures. At low temperature, $T_s = 310^\circ\text{C}$, alloys grow by island formation and there is minimal island–island interaction due to low surface diffusion. An intermediate substrate temperature of $T_s = 390^\circ\text{C}$ allows considerable opportunity for atoms and islands to interact with one another but not with the steps. This results in $2 \times n$ reconstruction of the alloy by formation of missing dimer rows. At $T_s = 470^\circ\text{C}$, the diffusion length of the atoms is larger than the average terrace width and they prefer to incorporate at the steps. Hence, the step flow is the main growth mechanism.

Acknowledgements

We thank S. Ciraci and J.B. Pethica for fruitful discussions. This work was supported by TUBITAK, The Scientific and Technological Research Council of Turkey, under the contract number TBAG-1094.

References

- [1] S.C. Jain, J.R. Willis and R. Bullough, *Adv. Phys.* 39 (1990) 127.
- [2] T.S. Kuan and S.S. Iyer, *Appl. Phys. Lett.* 59 (1991) 2242.
- [3] F.K. LeGoues, V.P. Kesan, S.S. Iyer, J. Tersoff and R. Tromp, *Phys. Rev. Lett.* 64 (1990) 2038.
- [4] D.E. Jesson, S.J. Pennycook, J.-M. Baribeau and D.C. Houghton, *Phys. Rev. Lett.* 68 (1992) 2062.
- [5] F.K. LeGoues, V.P. Kesan and S.S. Iyer, *Phys. Rev. Lett.* 64 (1990) 40.
- [6] S. Froyen, D.M. Wood and A. Zunger, *Appl. Phys. Lett.* 54 (1989) 484.
- [7] S.F. Nelson, K. Ismail, J.J. Nocera, F.F. Fang, E.E. Mendez, J.O. Chu and B.S. Meyerson, *Appl. Phys. Lett.* 61 (1992) 64.
- [8] Y.-J. Mii, Y.-H. Xie, E.A. Fitzgerald, D. Monroe, F.A. Theil, B.E. Weir and L.C. Feldman, *Appl. Phys. Lett.* 59 (1991) 1611.
- [9] F. Schaffler, D. Tobben, H.J. Herzog, G. Abstrieter and B. Hollander, *Semicond. Sci. Technol.* 7 (1992) 260.
- [10] S. Ciraci and I. Batra, *Phys. Rev. B* 38 (1988) 1835.
- [11] D.E. Jesson, S.J. Pennycook, J.Z. Tischler, J.D. Budai, J.-M. Baribeau and D.C. Houghton, *Phys. Rev. Lett.* 70 (1993) 2293; F.K. LeGoues, J. Tersoff and R.M. Tromp, *Phys. Rev. Lett.* 71 (1993) 3736; D.E. Jesson, S.J. Pennycook, J.Z. Tischler, J.D. Budai, J.-M. Baribeau and D.C. Houghton, *Phys. Rev. Lett.* 71 (1993) 3737.
- [12] J. Albers, *Phys. World* 7 (1994) 24.
- [13] Y.-W. Mo and M.G. Lagally, *Surf. Sci.* 248 (1991) 313.
- [14] R.J. Hamers, U.K. Kohler and J.E. Demuth, *J. Vac. Sci. Technol. A* 8 (1990) 195.
- [15] A.J. Hoeven, D. Dijkkamp, E.J. van Loenen, J.M. Lensinck and J. Dieleman, *J. Vac. Sci. Technol. A* 8 (1990) 207.
- [16] Y.-W. Mo, D.E. Savage, B.S. Swartzentruber and M.G. Lagally, *Phys. Rev. Lett.* 64 (1990) 1020.
- [17] J. Knall and J.B. Pethica, *Surf. Sci.* 265 (1992) 156.
- [18] A. Oral, PhD Thesis, Bilkent University (1994).
- [19] A. Oral and R. Ellialtıoglu, to be published.
- [20] Wacker Chemitronics GmbH, Germany.
- [21] A. Ishizaka and Y. Shiraki, *J. Electrochem. Soc.* 133 (1986) 666.
- [22] D.J. Chadi, *Phys. Rev. Lett.* 59 (1987) 1691.
- [23] M.G. Lagally, *Phys. Today* 11 (1993) 24.
- [24] R.A. Wolkow, *Phys. Rev. Lett.* 68 (1992) 2636.
- [25] K. Cho and J.D. Joannopoulos, *Phys. Rev. Lett.* 71 (1993) 1387.
- [26] R. Butz and S. Kempers, *Appl. Phys. Lett.* 61 (1992) 1307.
- [27] Xun Chen, Fang Wu, Zhenyu Zhang and M.G. Lagally, *Phys. Rev. Lett.* 73 (1994) 850.